1996MNRAS.280..806S

Mon. Not. R. Astron. Soc. **280,** 806–822 (1996)

The orbital dispersion of the macroscopic Taurid objects

D. I. Steel[1,2]★† and D. J. Asher[3]‡

[1]*Department of Physics and Mathematical Physics, University of Adelaide, SA 5005, Australia*
[2]*Anglo-Australian Observatory, Coonabarabran, NSW 2357, Australia*
[3]*Anglo-Australian Observatory, PO Box 296, Epping, NSW 2121, Australia*

Accepted 1995 December 18. Received 1995 November 29; in original form 1995 August 11

ABSTRACT

If the Taurid Complex asteroids (plus 2P/Encke) are derived from the fragmentation of a giant comet over the past 20–30 kyr, as we have suggested elsewhere, then we need to identify some mechanism which could cause the observed dispersion in semimajor axes ($1.8 < a < 2.6$ au), eccentricities ($0.64 < e < 0.85$), and longitudes of perihelion ($100° < \varpi < 190°$); the range in inclinations (i) is easily producible by secular perturbations. The problem devolves to one of identifying a source for the variations in a and e since, for a range of values of those parameters, differential precession will lead to a spreading in ϖ. Here we show that, considering only gravitational effects for variational orbits based on those of 2P/Encke, 5025 P-L and (6063) Jason, chaotic dynamical evolution over 30 kyr produces alterations in a and e which are insufficient to match the observed spread, suggesting that the asteroids concerned cannot have been derived from the splitting of a parent asteroid (i.e., inert object) on such a time-scale. However, plausible non-gravitational forces modelled quantitatively upon the observed motion of 2P/Encke can explain the spread, which may be interpreted as being supportive of our hypothesis of a cometary origin for the asteroids in the complex. Such forces also allow a connection with the Hephaistos group of objects to be made.

Key words: methods: numerical – celestial mechanics, stellar dynamics – comets: general – minor planets, asteroids.

1 INTRODUCTION

The Taurid complex (TC) of macroscopic objects (asteroids and comet 2P/Encke) is distinguished from other such objects on the grounds of having semimajor axes (a) in the range 1.8–2.6 au, eccentricities (e) in the range 0.64–0.85, low inclinations ($i \leq 12°$), and longitudes of perihelion in the range $100° < \varpi < 190°$ (Asher, Clube & Steel 1993a,b; Asher et al. 1994b; see also Napier 1993). This complex derives its name from the Taurid meteor showers, the meteoroids producing those showers having similar orbital characteristics (Štohl 1986; Steel, Asher & Clube 1991; Štohl & Porubčan 1992). For some decades it has been recognized that the stream responsible for these showers is a major contributor to the meteoroid/zodiacal dust population in the inner Solar system (Whipple 1967; Kresák 1980; Štohl 1986; Kresák & Kresáková 1987).

We update our last listing (Asher et al. 1994b) of TC macroscopic objects in Table 1, which contains all asteroids (and comets) selected from the discovered data base available in 1995 June on the basis of orbital parameters (a, e, i) such that a discriminant D has a value less than or equal to 0.2, D being defined by

$$D^2 = \left(\frac{a_1 - a_2}{3}\right)^2 + (e_1 - e_2)^2 + \left(2 \sin \frac{i_1 - i_2}{2}\right)^2, \quad (1)$$

where the subscript 1 denotes the test orbit, and the subscript 2 denotes an orbit taken from the lists of known near-Earth asteroids (NEAs) and Earth-crossing comets. The test orbit used here is defined by the observed Taurid meteors, with $a_1 = 2.1$ au, $e_1 = 0.82$, and $i_1 = 4°$ (Steel et al. 1991). The NEA orbital parameters used are the osculating values for a (which are broadly constant under secular perturbations), but the maximum values of e and the minimum values of i which are attained under secular perturbations;

★E-mail: dsteel@physics.adelaide.edu.au
†Present address: Department of Physics and Mathematical Physics, University of Adelaide, SA 5005, Australia.
‡Present address: National Astronomical Observatory, Mitaka, Tokyo 181, Japan.

© 1996 RAS

© Royal Astronomical Society • Provided by the NASA Astrophysics Data System

1996MNRAS.280..806S

this corresponds closely to the circumstances under which the Taurid meteors are observed (i.e., the part of the orbital evolution placing a node near 1 au: e and i are linked in antiphase). This criterion gives equal weight to orbital element differences of $\Delta a \simeq 0.3$ au, $\Delta e \simeq 0.1$ and $\Delta i \simeq 6°$, the above definition in essence defining an ellipsoid in (a, e, i)-space. Other definitions could be espoused (for example, separate limits on a, e and i), but we have found this selection criterion to be suitable for our purposes.

There are 25 NEAs in Table 1, and of these 15 are identified as being aligned with the Taurid meteors (longitudes of perihelion in the range $100° < \varpi < 190°$), whilst five others plus D/Helfenzrieder (1766 G1; Marsden & Williams 1995) appear to form another concentration which we choose to identify with the largest asteroid in the group, (2212) Hephaistos (see Asher et al. 1993a, 1994b, and Steel & Asher 1994). The remaining five are members of neither group; we note, however, that (2101) Adonis and the small asteroid 1995 CS form a pair which is worthy of investigation, especially since (2101) Adonis has previously been suggested as being linked to various meteor showers, including the α Capricornids (Babadzhanov & Obrubov 1992).

All orbits in Table 1 are shown in Fig. 1, their paths being projected on to the ecliptic plane, along with the orbits of the Earth and Jupiter.

Based on a null hypothesis that one might expect ϖ to be randomly distributed, finding 15 out of 25 NEAs with similar parameters (a, e, i) within a pre-defined 90° band in ϖ has a probability of occurrence of 0.000 215; alternatively, we could include also the comets in Table 1, the required probability then being that for finding 16 out of 27 in that band, that probability being 0.000 162. In view of the slimness of these probabilities it is likely that the values of ϖ are *not* randomly distributed, and this requires an explanation. The explanation that we favour is that the TC objects are the remnants of a giant cometary object that has broken up over the past 20–30 kyr, as suggested by Clube & Napier (1984, 1986; see also Clube 1987); Kresák (1980) mentioned that 2P/Encke and the Taurids may have been produced by a Chiron-like progenitor. That time-scale is based upon considerations of the dispersion of the TC meteoroids (Steel et al. 1991). A minimum time-scale of 18 kyr has been set by the identification of three distinct sets of four meteor showers (i.e., daytime and nighttime for both ascending and

Table 1. Macroscopic objects identified through their difference $D(a, e, i) \leq 0.20$ from a reference orbit defined by Taurid meteors (see text; this form of analysis was also extensively discussed by Asher et al. 1994b). The osculating elements for each are listed below: a is the semimajor axis and q the perihelion distance, both in au; e is the eccentricity; i is the inclination to the ecliptic and ϖ the longitude of perihelion, both in degrees. H is the absolute magnitude for each asteroid, and d the equivalent diameter in km for an assumed albedo $p = 0.08$, calculated using the expression of Rowe (1993); see fig. 2(d) in Steel (1995) for values of d for different albedos. The 15 asteroids (plus 2P/Encke) with longitudes of perihelion in the range $100° < \varpi < 190°$ are placed in the column headed 'Aligned with Taurids'. We have previously identified a second alignment of five asteroids (plus D/Helfenzrieder) in the range $220° < \varpi < 260°$ (Steel & Asher 1994); these appear in the column headed 'Hephaistos group'. Five other asteroids (four of them being recent discoveries) fall into neither of these apparent alignments; we note that (2101) Adonis and 1995 CS form a very similar pairing which may be significant, especially since the former is suspected of being the parent of various meteor showers (Babadzhanov & Obrubov 1992).

Aligned with Taurids	Hephaistos group	Others	H	d	a	q	e	i	D	ϖ
	1991 AQ		17.0	1.9	2.22	0.49	0.78	3	0.06	222
	(2212) Hephaistos		13.8	8.1	2.17	0.36	0.83	12	0.06	237
1993 KA_2			29.0	0.007	2.23	0.50	0.77	3	0.06	141
(6063) Jason			15.1	4.5	2.22	0.52	0.76	5	0.07	146
		1995 EK_1	18.0	1.2	2.26	0.51	0.78	9	0.10	292
		1995 CS	25.0	0.047	1.90	0.44	0.77	3	0.10	28
		(2101) Adonis	18.7	0.85	1.87	0.44	0.76	1	0.10	33
1991 TB_2			17.0	1.9	2.40	0.39	0.84	9	0.10	133
(2201) Oljato			15.3	4.1	2.18	0.63	0.71	3	0.12	173
	1990 SM		16.5	2.3	2.12	0.49	0.77	12	0.12	244
(5143) Heracles			13.9	7.7	1.83	0.42	0.77	9	0.13	177
		1994 XD	19.0	0.74	2.36	0.64	0.73	4	0.13	345
5025 P–L			15.9	3.1	2.14	0.65	0.70	3	0.13	136
(4197) 1982 TA			14.5	5.9	2.30	0.52	0.77	12	0.14	129
1995 FF			26.5	0.023	2.34	0.67	0.71	1	0.14	109
1991 BA			28.5	0.009	2.24	0.71	0.68	2	0.16	190
(4341) Poseidon			15.6	3.5	1.84	0.59	0.68	12	0.16	124
	(4486) Mithra		15.4	3.9	2.20	0.74	0.66	3	0.17	251
1994 AH_2			16.5	2.3	2.53	0.73	0.71	10	0.17	189
	1990 TG_1		15.0	4.7	2.48	0.76	0.69	9	0.18	238
		1994 EK	20.0	0.47	2.14	0.77	0.64	6	0.19	72
(5731) Zeus			15.5	3.7	2.26	0.79	0.65	12	0.19	138
1991 GO			19.0	0.74	1.96	0.66	0.66	10	0.19	114
(4183) Cuno			14.5	5.9	1.98	0.72	0.64	7	0.19	171
1990 HA			17.0	1.9	2.58	0.79	0.69	4	0.20	133
2P/Encke					2.21	0.33	0.85	12	0.05	161
	D/Helfenzrieder				2.66	0.41	0.85	8	0.20	255

© Royal Astronomical Society • Provided by the NASA Astrophysics Data System

1996MNRAS.280..806S

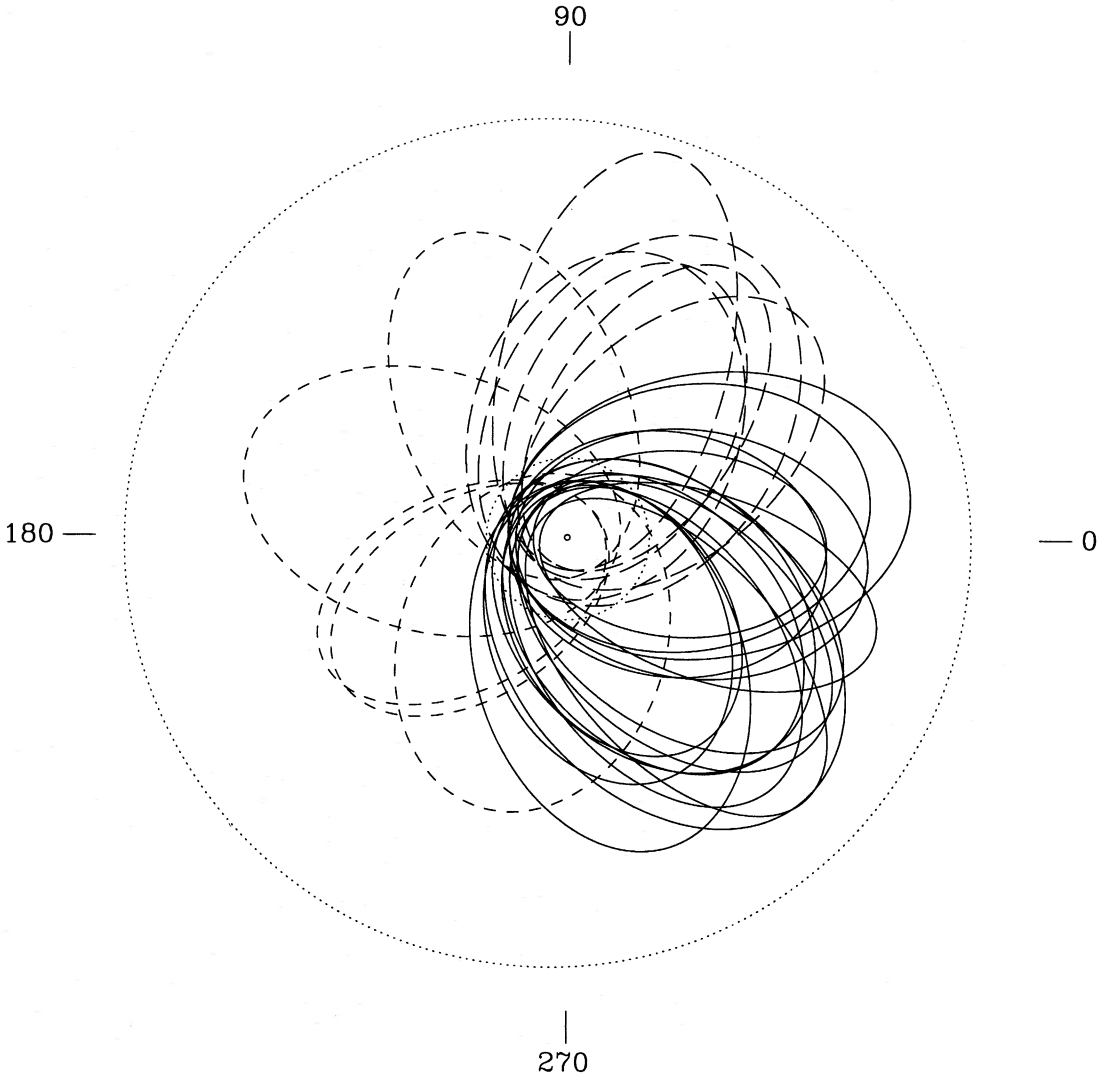

Figure 1. The orbits of all objects listed in Table 1, projected on to the ecliptic plane. The orbits of the Earth and Jupiter are shown as dotted lines. The 16 Taurid Complex objects are plotted as solid lines, the six Hephaistos group objects as long-dashed lines, and the other five objects (all asteroids) as short-dashed lines. As indicated by the numbers, longitude increases anticlockwise (i.e., this is a view from north of the ecliptic), the origin being towards the right.

descending nodes) by Babadzhanov, Obrubov & Makhmudov (1990; see also Babadzhanov & Obrubov 1992 and Štohl & Porubčan 1992), the separation being due to the precession in the longitude of perihelion (ϖ) during each precession cycle in the argument of perihelion (ω), and hence the showers occurring at different nodal longitudes (Ω), or times of year. The time-scale derives from the elapsed period necessary to allow three precession cycles in ω, characteristic times for each cycle having been conveniently tabulated by Asher & Clube (1993; see their table A1, which presents rotation periods for ω and ϖ for a matrix of TC a and e values). Over 20–30 kyr the *dispersion* in ϖ attained between orbits in the range $a = 1.8$–2.4 au is $\sim 90°$, and if the TC age is $\lesssim 30$ kyr, then there has been insufficient time for a complete rotation of ϖ (except perhaps for the very largest orbits: $a = 2.5$–2.6 au). This is not inconsistent with an earlier investigation of the Taurid meteoroid stream by Jones (1986), since he used different criteria to assess the time-scale, derived a value of order 100 kyr. If the stream was formed as long ago as that, then there would have been 10–20 precession cycles in ω, each producing meteor shower quadruplets, so that a whole series of Taurid-type showers would be expected to occur, spread throughout the year. Their apparent non-observation leads us to choose 20–30 kyr as the period over which the progenitor of the TC has been disintegrating in the inner Solar system, and not 100 kyr. The difference is very important: it will be seen below that gravitational perturbations alone cannot produce within 30 kyr the dispersion in orbital elements observed in the TC asteroids, whereas it is conceivable that such perturbations could be responsible if 100 kyr were allowed. Thus, if these asteroids are indeed derived from the break-up of a giant body which also produced the Taurid meteoroids, then their orbital dispersion requires the action of non-gravitational forces, implying a cometary origin.

We note here that an alternative explanation for the non-random values of ϖ in the TC asteroids (only: not the

© Royal Astronomical Society • Provided by the NASA Astrophysics Data System

1996MNRAS.280..806S

Hephaistos group) was postulated by Klačka (1995). We have rebutted Klačka's argument elsewhere (Steel et al. 1996), showing that it was based upon an invalid application of the secular perturbation theory of Brouwer & van Woerkom (1950). Nevertheless, it is important to acknowledge that the giant comet hypothesis is not the only explanation which might fit the observations, and the possibility that some form of selection effect has led to the apparent alignment of the objects that we call the Taurid Complex should certainly be entertained. Indeed, Valsecchi (1995, personal communication) has indicated that, along with coworkers, he has identified a discovery selection effect that might provide an alternative explanation for the apparent asteroid alignment in Table 1, the alignment with 2P/Encke and the Taurid meteoroids then being assumed to be a coincidence.

In contrast with the effort of Klačka, Valsecchi et al. (1995) have investigated, using numerical integrations, the orbital evolution under gravitational perturbations of macroscopic objects with orbits similar to 2P/Encke, having been prompted by some of our earlier work. They state that 'We find that the secular dynamics, and in particular the secular resonances, are sufficient to explain the existence of many bodies on Encke-like orbits, coming from the main asteroid belt and from the Jupiter family of comets; from a dynamical point of view the existence of a large parent body is therefore no longer necessary.' Here we must state that we welcome the work by Valsecchi et al. (1995) as being a valuable contribution to the investigations of this subject, but we differ strongly with part of the statement quoted here, and implied elsewhere in their paper. What Valsecchi et al. (1995) accomplished was to show how orbits with (a, e, i) similar to 2P/Encke (i.e., orbits like those we list in Table 1) could come about on a time-scale of order 1 Myr; however, they did *not* show why the observed orbits are apparently non-random in ϖ. This question, which was the source of the original suggestion of a large parent body – a giant comet – for the TC is not investigated (but is mentioned) by Valsecchi et al. (1995); see the discussion below in Section 3.1.

It is regrettable that colours and hence compositional classifications are not yet available for most of the TC asteroids (nor, indeed, most NEAs), meaning that there is a dearth of physical evidence to support the dynamical analysis which is the subject of the present paper. However, in passing we note that there is *some* physical evidence that supports our hypothesis that the TC objects comprise a genetically linked group. In Fig. 2 we have plotted the absolute magnitude (H) for all known Earth-crossing asteroids (ECAs, defined here as being all those with $q < 1.0167$

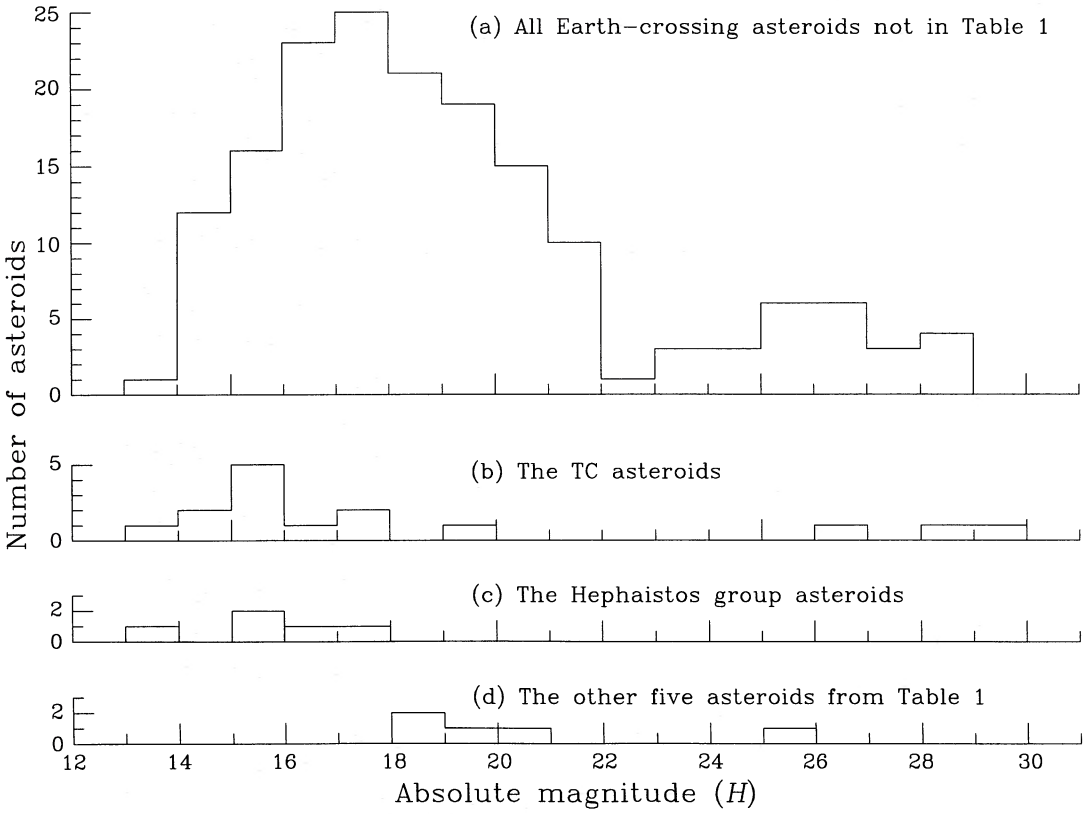

Figure 2. The absolute magnitude distribution for all Earth-crossing asteroids known as of 1995 June. The top plot (a) is for all such asteroids except for those appearing in Table 1. The 25 asteroids in Table 1 are plotted here as (b) TC asteroids, 15 total; (c) Hephaistos-group asteroids, five total; (d) other asteroids, five total. The fact that (b) and (c) have peaks at brighter magnitudes argues for a physical differentiation between the members of those groups and the general Earth-crossers in plot (a); the fact that the magnitudes in plot (d) are fainter on average than those in any of the other three plots negates any suggestion that (b) and (c) are intrinsically brighter/larger due to some selection effect depending upon their orbital parameters, since the orbits for groups (b), (c) and (d) are similar. Also noteworthy is the existence of three very faint/small asteroids in the TC group, which again may be interpreted in terms of a cometary break-up origin.

© Royal Astronomical Society • Provided by the NASA Astrophysics Data System

1996MNRAS.280..806S

au) known in 1995 June. Four separate plots are shown. The uppermost plot (Fig. 2a) consists of all ECAs except the 25 listed in Table 1; this distribution appears to be bimodal, with the major peak at $H=17$–18 and a subsidiary peak at $H=25$–27. The faint asteroids ($H>22$) are discoveries made by *Spacewatch* (Rabinowitz 1993); very few such orbits are yet known from the very large population that exists in Earth-approaching orbits. The other three plots (Figs 2b–d) comprise (b) the 15 TC asteroids, (c) the five Hephaistos group asteroids, and (d) the other five asteroids in Table 1. The TC asteroids show a distinct peak at $H=15$–16 (i.e., 2 mag brighter than that for other ECAs, Fig. 2a), but with a notable tail of faint/small bodies at $H>26$. The Hephaistos group is small in membership, but nevertheless it seems clear that these are brighter/larger than the ECA norm. One might explain this contrast between Figs 2(b), (c) and Fig. 2(a) on the grounds of a simple selection effect – such high-e orbits as those in Table 1 perhaps having larger angular speeds on average than the other ECAs, hence needing to be intrinsically brighter in order to be discovered – were it not for Fig. 2(d): the five asteroids in that plot have similar orbital characteristics as those in Figs 2(b) and (c), but they are fainter, on average, than both (i) the TC and Hephaistos asteroids, and (ii) the other ECAs. We interpret Fig. 2(b) as being evidence for a giant comet break-up, with most of the mass being held in the large fragments, but with some small asteroids/large meteoroids occupying similar orbits; note that Rabinowitz (1993) also has argued that the small *Spacewatch* discoveries could be cometary fragments. It may well be that the Hephaistos group will eventually be shown to contain small asteroids, too, but at present the count statistics are so low (the TC asteroids showing a 4:1 large:small ratio in their observed population) that it is not surprising that no small Hephaistos-group objects have been found yet.

The only comet found so far in the Taurid Complex is 2P/Encke, which has long been linked with the Taurid meteors (Whipple 1940; Whipple & Hamid 1952; Štohl 1986; Sekanina 1991; Štohl & Porubčan 1992); its activity in the present epoch might be due to it having the smallest perihelion distance of the macroscopic objects yet identified, the others then being thought of as extinct or dormant comets.

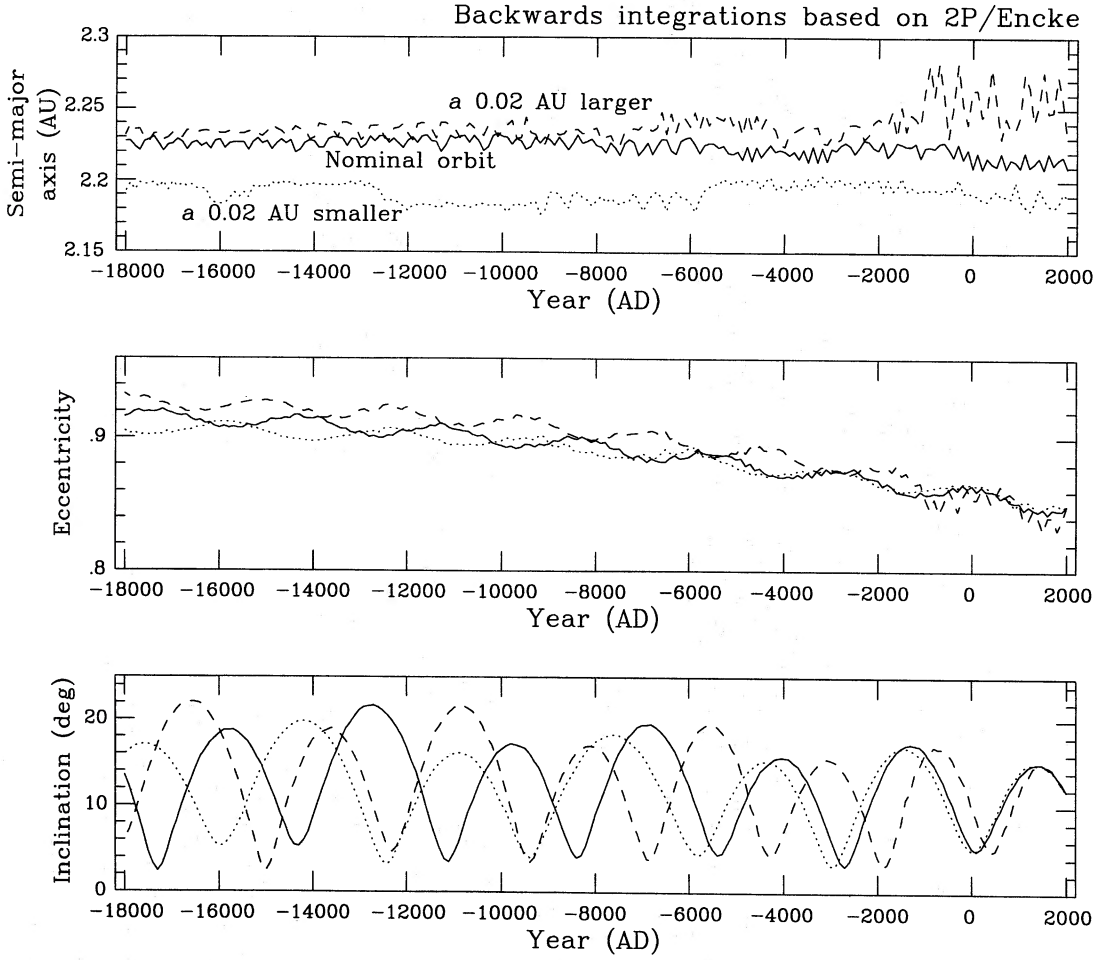

Figure 3. Results of a backwards integration over 20 kyr of three orbits based upon the elements of 2P/Encke. The nominal orbit (solid line) has start elements identical to those of that comet, while the other two orbits have only the initial value of the semimajor axis altered to be 0.02 au smaller (dotted line), and 0.02 au larger (dashed line), than the nominal orbit. Whilst secular perturbations of these orbits produce variations in the inclination sufficient to explain the spread in this parameter in the observed Taurid objects (Table 1), this is not the case for the semimajor axes or eccentricities.

© Royal Astronomical Society • Provided by the NASA Astrophysics Data System

1996MNRAS.280..806S

A necessary step in advancing this hypothesis of a giant comet origin for the TC asteroids is an explanation of the dispersion in a, e and ϖ which is seen (i varies sufficiently under secular perturbations to encompass the TC spread, as shown in Section 2.1). The observed spread in ϖ will result, on an appropriate time-scale, from the differential precession of NEA orbits having the given spread in a and e; so the problem reduces to one of finding a mechanism which will cause sufficient (a, e) dispersion. In Section 2.2 we show that, considering only gravitational perturbations for variational orbits of 2P/Encke, chaotic dynamical evolution over 30 kyr leads to a spread in a of $\sim$0.08 au and $\sim$0.08 in e, and thus $\sim$25° in ϖ. Such perturbations are insufficient to match the observed TC spread. A similar treatment for 5025 P-L renders a spread of 0.25 au in a, 0.16 in e, and thus $\sim$100° in ϖ, which is adequate for ϖ but not for a and e. For (6063) Jason the spreads are 0.2 au in a, 0.06 in e, and 60° in ϖ. These results suggest that the asteroids concerned cannot have been derived from the splitting of a single parent asteroid (meaning, an inert object) on such a time-scale. On the other hand, in Section 3 we investigate plausible non-gravitational forces, modelled upon the observed motion of 2P/Encke, and find that these can explain the spread, lending support to the hypothesis that a disintegrating giant comet produced the Taurid Complex.

2 GRAVITATIONAL EFFECTS

The results we present here are derived from numerical integrations of the type described previously by us in connection with our investigations of the orbital evolution of planet-crossing asteroids (5145) Pholus (Asher & Steel 1993), (5335) Damocles (Asher et al. 1994a), and also some of the TC asteroids (Asher et al. 1993a). Previous experience gained both by ourselves and by other researchers (e.g. Milani et al. 1989; Hahn & Bailey 1990; Levison & Duncan 1994) has shown that infinitesimal changes to the start parameters for any specific orbital integration can lead to radical differences in the end result, particularly due to the changed circumstances of planetary close encounters. Even with identical start parameters, the results obtained will change if the same code is run on another machine. Thus no significant advantage is obtained by integrating the orbits of the planets (which would increase the execution time by about an order of magnitude), and so we have used the 500-yr average elements generated by Quinn, Tremaine & Duncan (1991).

The main point of this section of the paper is to show that the effect of random close planetary encounters are insufficient over 30 kyr to produce the observed orbital dispersion of the TC objects. Before discussing these chaos-producing

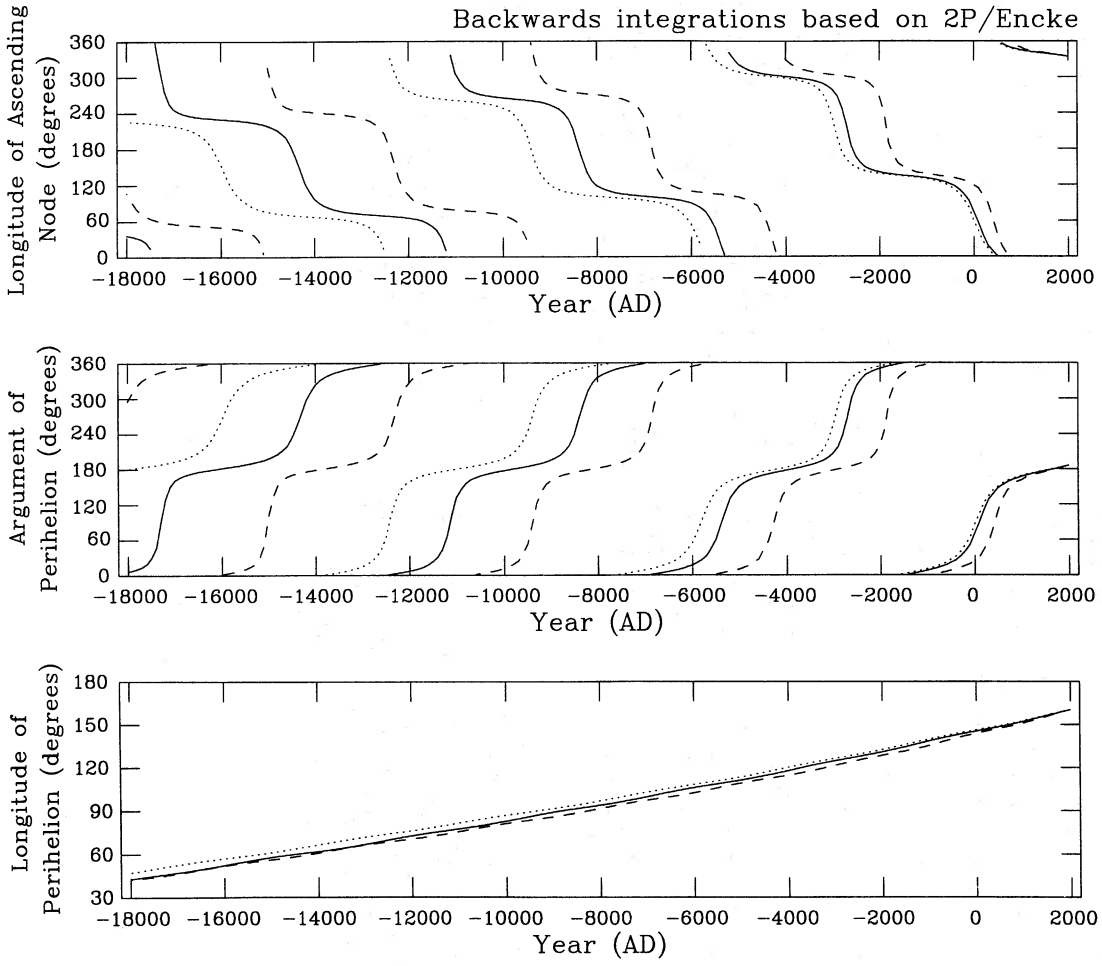

Figure 4. As Fig. 3, except for the longitude of the ascending node, the argument of perihelion, and the longitude of perihelion.

© Royal Astronomical Society • Provided by the NASA Astrophysics Data System

1996MNRAS.280..806S

encounters, however, we first consider the effects of secular variations in e and i, and whether these can explain the observed spread in those parameters within the TC asteroids.

2.1 Effect of secular perturbations upon the eccentricity and inclination

A comparison between the secular perturbations theory of Brouwer (1947) and numerical integrations was carried out by Asher & Clube (1993) for the present-day elements of 2P/Encke followed back over 10 kyr. Brouwer developed this theory specifically for dealing with 2P/Encke, its eccentricity being too high for the application of the theory which he had developed for main belt asteroids, that work culminating in the publication by Brouwer & vanWoerkom (1950); Klačka (1995) erroneously applied the Brouwer & van Woerkom low-e theory to the high-e TC asteroids. The comparison by Asher & Clube (1993) of the results of numerical integrations with the Brouwer theory indicated that close agreement is obtained (see fig. A2 of that paper), although we should note here that Jupiter was assumed to be in a circular orbit; also note, in connection with that figure, that the angular elements plotted were referred to the orbital plane of Jupiter, so that the inclination plot does not show the minima (referred to the ecliptic) that would actually result. For present purposes, we merely note that the results of Asher & Clube (1993) indicate that oscillations in i of sufficient amplitude occur under solely secular perturbations so as to explain the range observed in the TC (Table 1), but the oscillations in e, which are in counterphase with those in i, are of insufficient amplitude to provide a ready explanation for the observed TC spread. We acknowledge, however, that no secular trend in e is seen in those results, and that is due to the assumed circularity of the Jovian orbit. Thus we need to perform numerical integrations using the real planetary orbits (values from Quinn et al. 1991) in order to ascertain the real secular perturbations. We have previously performed backwards integrations over 20 kyr for some of the TC asteroids (Asher et al. 1993a), showing that whilst a does not vary appreciably (as expected), there are strong oscillations in e (and hence q), and also in i. Another lesson from that work was the need to include the terrestrial planets in any integration rather than just Jupiter and Saturn, or all four Jovian planets: this is because it is the close approaches to the terrestrial planets that cause rapid transition into chaotic orbital evolution. Michel, Froeschlé & Farinella (1996) have come to a similar conclusion, having conducted numerical integration experiments on the orbit of (4179) Toutatis.

Here we have integrated backwards in time over 20 kyr three hypothetical particles with start parameters based upon the orbit of comet 2P/Encke, as calculated by Nakano (1994). One particle was given the nominal orbit of 2P/Encke, whilst the other two had identical start parameters except with the semimajor axes varied by ± 0.02 au. Their semimajor axes (epoch 1997 June 01.0) were therefore 2.1895, 2.2095 and 2.2295 au. The results for a, e and i are shown in Fig. 3, and for Ω, ω and ϖ in Fig. 4. The choice of the semimajor axis as the parameter for adjustment between these three orbits was dictated by the desire to illustrate how secular perturbations can explain the spread in i within the TC objects (oscillations with full amplitude $\sim 20°$), because these oscillations in i (and thus e also) soon lapse out of phase for small initial orbital differences. This can be clearly seen in Fig. 3. Other points to note are as follows.

(i) The initial spread of ± 0.02 au in a is amplified by a factor of about 3 at times through the vagaries of close encounters (note that the larger orbit spends some time in the first 4 kyr of the backwards integration in the proximity of the 7:2 Jovian mean motion resonance at $a = 2.256$ au; cf. Asher & Clube 1993), but this is far from sufficient to fit the $1.8 < a < 2.6$ au spread observed, and the spread in ϖ (under 10°) is also too small.

(ii) Two oscillations in e and i occur for each rotation of ω. These are sometimes referred to as the Kozai cycles, after the work of Kozai (1962). The rotation period for ω is 5–7 kyr, in agreement with table A1 of Asher & Clube (1993). Also in agreement with the contents of that table is the fact that ϖ rotates through $\sim 120°$ in 20 kyr, indicating a period for full rotation of ~ 60 kyr.

(iii) There is a secular decrease in e from 20 kyr ago until the present, this being due to the longitudes of aphelion of the particles moving towards the longitude of perihelion of Jupiter, which rotates with a much longer period, about 300 kyr (Quinn et al. 1991). Thus, although e reduces from a maximum value of about 0.93 to a minimum value of around 0.83, at any particular time the spread among these three particles is only 0.03 at most. This would continue to be the case until such time as there is substantial dispersion in ϖ (since the longitude of perihelion is just the longitude of aphelion plus 180°). Therefore we find that secular perturbations alone cannot be responsible for the observed divergence in the TC eccentricities.

Note that in this 20-kyr backwards integration it might be imagined from Fig. 3 that e increases monotonically going backwards in time so as to reach unity [the object falling into – or seeming to emerge from, given the direction of the arrow of time! – the Sun, as illustrated by Farinella et al. (1994) and Levison & Duncan (1994)], but later results presented in Figs 5, 7 and 9, from 30-kyr integrations, show that e does eventually start to decrease again going backwards in time. Thus, while Sun-grazing has been demonstrated as a real phenomenon by those authors, it does not happen to TC orbits during the time (the past ~ 30 kyr) over which the Taurid meteoroid complex has formed.

2.2 Effect of chaotic dynamics on the semimajor axis and longitude of perihelion

Having obtained some indication of the effects of random close planetary encounters from the results plotted in Figs 3 and 4, we next investigate a larger set of variational orbit integrations. As starting points for these integrations we used three reference orbits. The first was the nominal orbit of 2P/Encke, as used in Section 2.1. The second was the orbit of 5025 P-L due to E. Bowell (cf. Table 1); this asteroid was chosen since it is close to the centre of the spread of the TC asteroids. Its short observed arc means that its orbit is not secure and the asteroid has been lost, but it is a suitable basis for the present numerical experiments. We also

© Royal Astronomical Society • Provided by the NASA Astrophysics Data System

1996MNRAS.280..806S

wanted to use a well-defined (numbered) asteroid orbit, and chose (6063) Jason as the third source orbit.

For each of these three orbits we performed a backwards integation over 30 kyr, and used the orbital parameters derived for that epoch as the bases for sets of forward integrations to the present. These forward integrations used in each case identical initial element sets apart from the mean anomaly (M), 18 hypothetical particles being invented with values of M spaced by 20° (cf. Jones 1986). Owing to the chaotic nature of such integrations through close planetary encounters (and, in reality, other effects such as the non-gravitational forces discussed in Section 3), these forward integrations result in contrasting evolutionary tracks being followed to the present.

For the integration results presented in Section 2.1 (Figs 3 and 4) we wanted to show the effect of short-term (10^2–10^3 yr) variations in the elements, and therefore output values every century. For the purposes of this section, however, we are mainly interested in the eventual dispersion attained (after 3×10^4 yr), and so we output the elements only every millennium (see Figs 5–10).

We first examine the results for the 18 particles based on

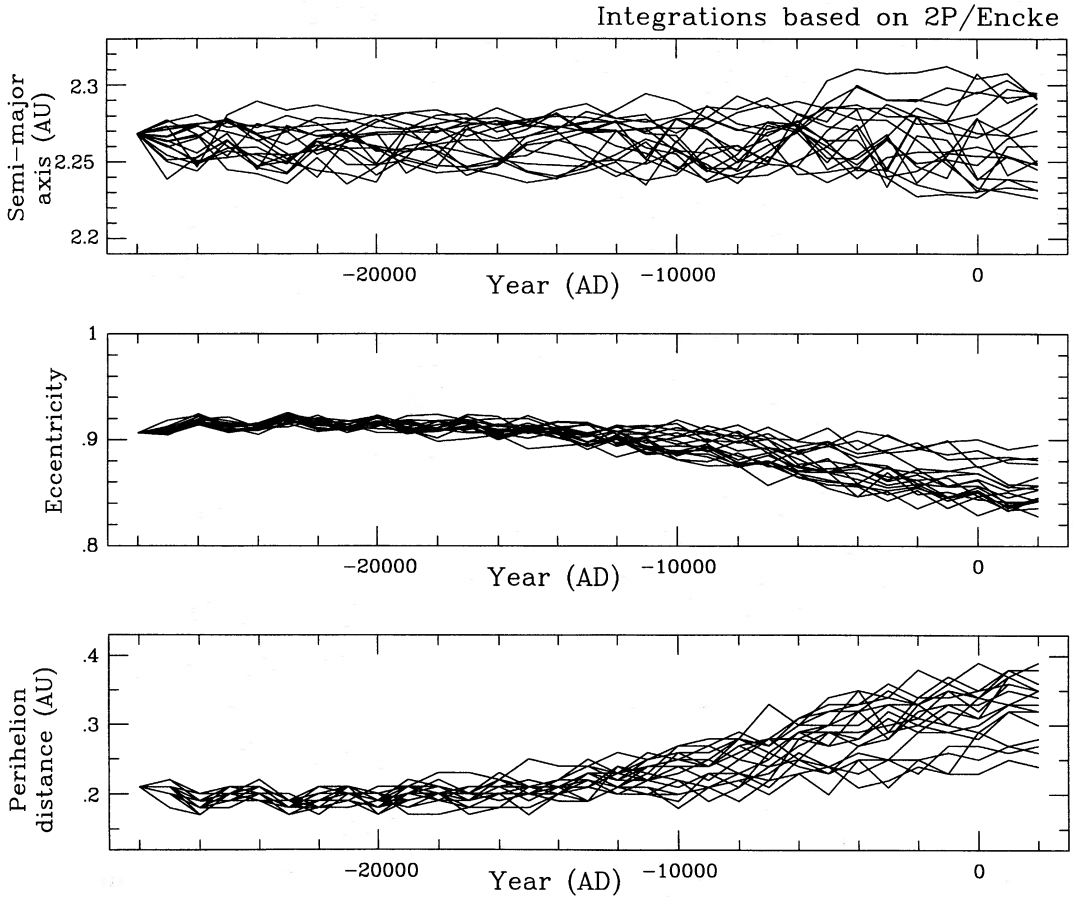

Figure 5. Results of the integration of the 18 particles in the Encke bundle, obtained from a backwards integration of 2P/Encke over 30 kyr, the elements in that epoch then being used for each of the 18 test particles except that values of the mean anomaly M are arbitrarily spaced by 20°. The significant point here is that the spreads in these elements are insufficient to match the observed spread in the TC orbits.

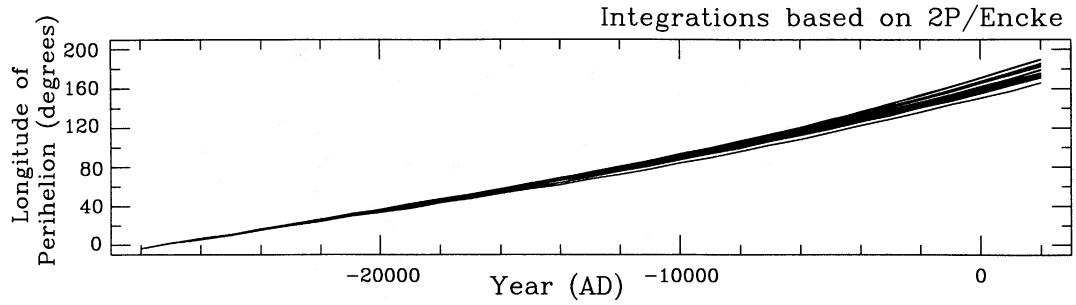

Figure 6. Values for the longitudes of perihelion (ϖ) as a function of time for the Encke bundle of 18 orbits, other elements of which were plotted in Fig. 5. The dispersion of ~30° obtained is too small to account for the observed spread in the TC objects.

© Royal Astronomical Society • Provided by the NASA Astrophysics Data System

1996MNRAS.280..806S

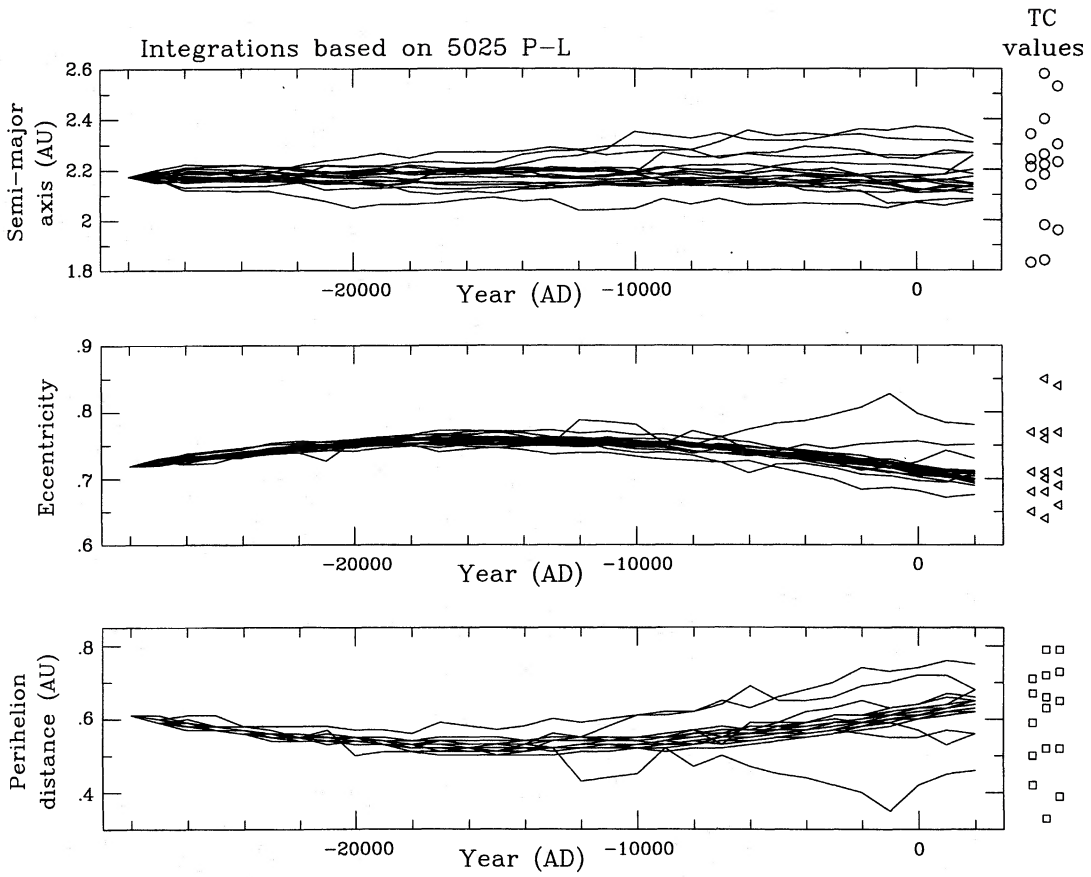

Figure 7. As Fig. 5, except for the 18 particles in the 5025 P-L bundle. The scales of the axes were chosen so as to cover the full range of each orbital element in the TC objects listed in Table 1. At the right of each plot symbols are set out so as to show the actual values of a, e and q for the 15 TC asteroids plus 2P/Encke. The sideways scatter of these symbols has no physical significance, merely resulting from offsets being applied so as to avoid symbol overprinting.

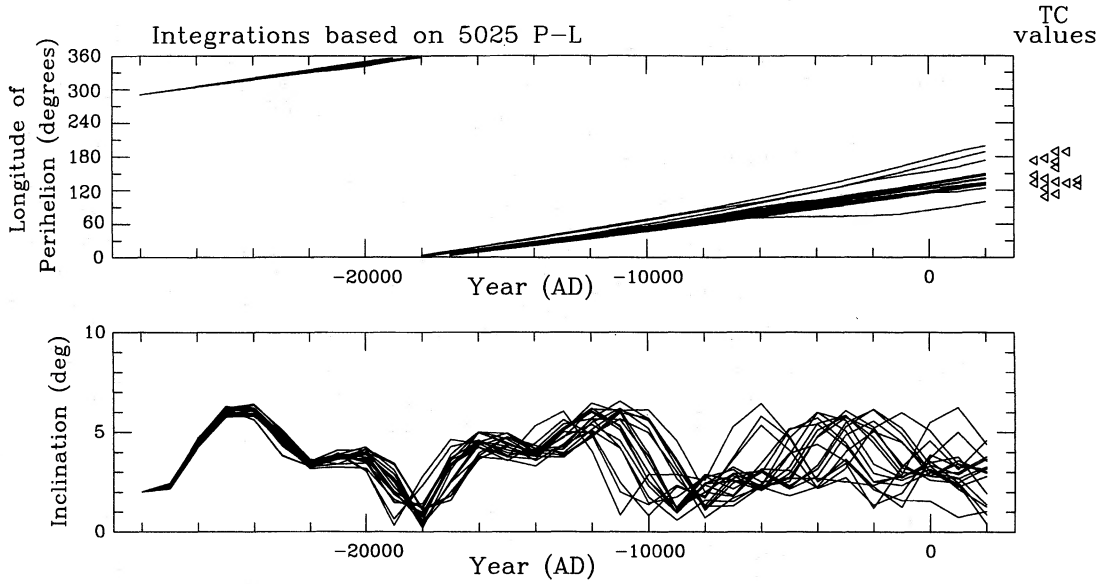

Figure 8. The upper plot is the equivalent to Fig. 6 except for the 18 particles in the 5025 P-L bundle. Four wayward particles out of the 18 produce a full range of 100°–200°, sufficient to cover the TC spread shown by the symbols at the right, but 14 of the 18 particles remain in a band at $120° < \varpi < 150°$. The lower plot shows the evolution of the orbital inclinations of these particles, with much smaller variations than those obtained for Encke-like particles (lower plot of Fig. 3). Since the 5025 P-L bundle remains at low inclinations, these particles have rather more frequent close encounters with the terrestrial planets, resulting in major orbital changes and hence outliers like the four disparate particles in the upper plot here, and in Fig. 7.

© Royal Astronomical Society • Provided by the NASA Astrophysics Data System

1996MNRAS.280..806S

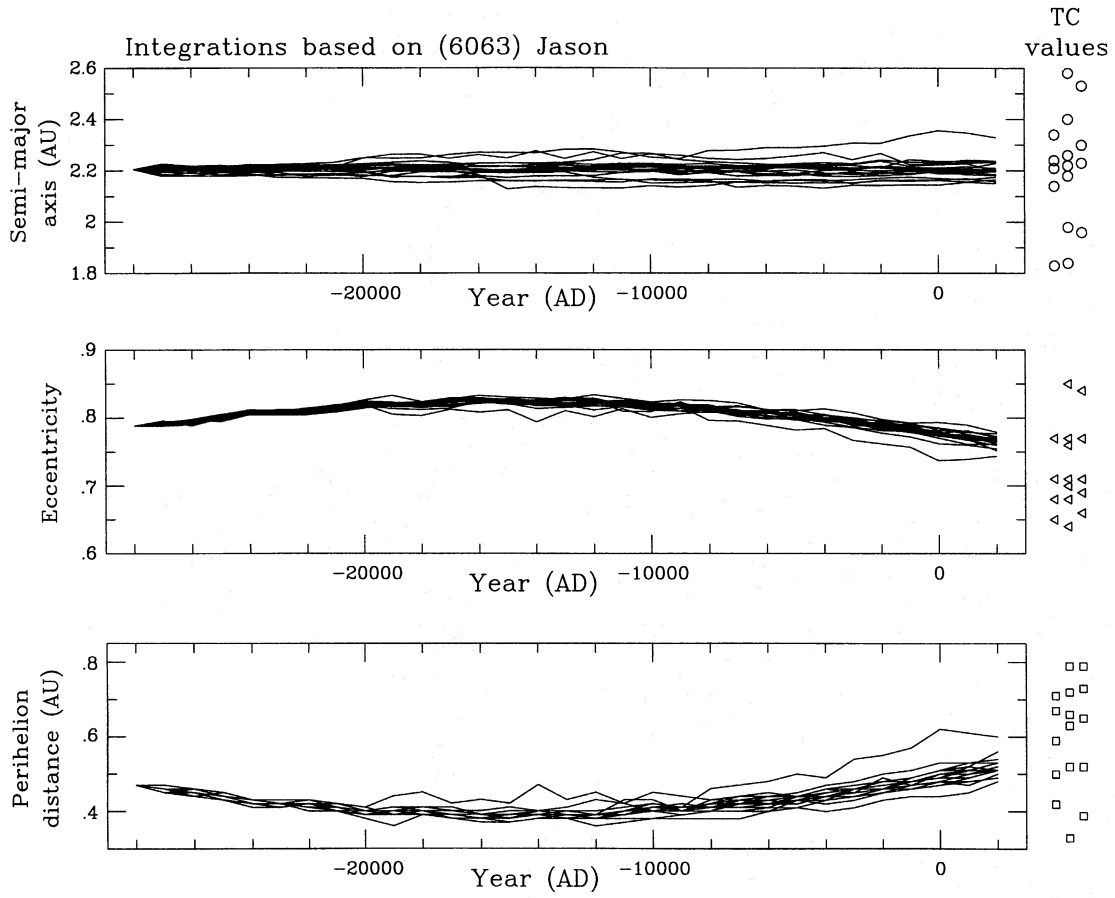

Figure 9. As Fig. 7, except for the 18 particles in the (6063) Jason bundle. One wayward particle out of the 18 is largely responsible for the range of parameters attained by the end of the integration; the rest remain tightly grouped.

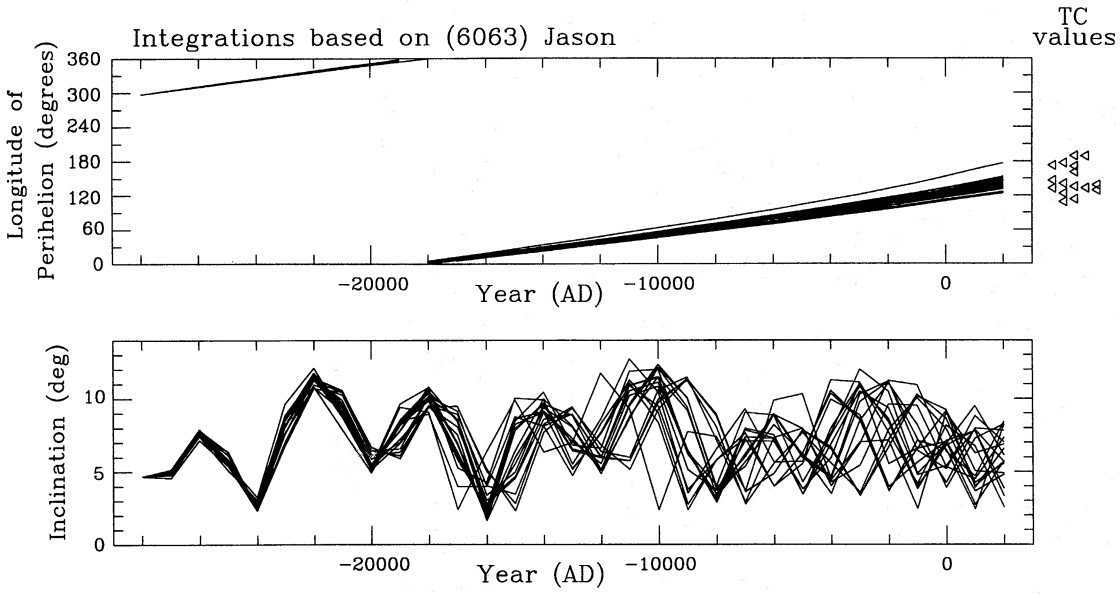

Figure 10. As Fig. 8, except for the 18 particles in the (6063) Jason bundle. The one wayward particle is responsible for over 40 per cent of the spread in ϖ, the rest remaining at $120° < \varpi < 155°$ at the end of the integration. Despite the small spread in the other orbital parameters, the cyclic variations in i soon get out of phase.

© Royal Astronomical Society • Provided by the NASA Astrophysics Data System

1996MNRAS.280..806S

2P/Encke, which we will refer to as the 'Encke bundle'. In Fig. 5 we plot the time evolution of the parameters a, e and q for the Encke bundle. The dispersion in each of these elements is seen to increase with time, especially over the last 10 kyr of the integrations, with total spreads attained being about 0.08 au in a, 0.08 in e, and 0.15 au in q. None of these spreads is large enough to match the observed TC dispersion in elements (Table 1 and Fig. 7). The divergence attained in ϖ (Fig. 6) is about 30°, only around one-third of the observed spread in the TC.

It is of interest to note that 2P/Encke has $\varpi = 161°$ (Table 1), whereas all 18 particles in the Encke bundle, resulting from a backwards and then forwards integration of hypothetical orbits based upon that comet, have $\varpi > 161°$ (Fig. 6). This is due to an effect of a non-repeated chance close encounter in the single backwards integration phase.

We now move on to the 18 particles based on 5025 P-L, the '5025 P-L bundle'. The results for a, e and q are shown in Fig. 7. It is immediately apparent that the dispersion obtained in each element is somewhat higher than in the case of the Encke bundle, although (i) the spread is still insufficient to match the observed distributions, and (ii) a few particles are responsible for much of the divarication. Regarding the dispersion, that achieved in a (~ 0.25 au) is about 30 per cent of that apparent in the TC objects, as much as 60 per cent of that needed in e (due to the singular evolution path of one object, that reaching $e > 0.8$ about 3 kyr ago), and comes close to reaching that required in q. We note, however, that in each elemental plot the majority of the particles remain closely correlated, following a similar path in e due to the domination of secular perturbations. Turning to the longitude of perihelion, we find (Fig. 8) that the 5025 P-L bundle produces a spread adequate to fit the TC values (actually giving a range of 100°–200°), but 14 of the 18 particles remain in a band at $120° < \varpi < 150°$; note that the present value of ϖ for 5025 P-L is 136°, in the centre of this band.

If it were not for the four wayward particles in the 5025 P-L bundle, the results would be broadly similar to those obtained for the Encke bundle. We must therefore address the question of the origin of this waywardness. For elements derived from those of 2P/Encke, the inclination oscillates under secular perturbations with a full amplitude of $\sim 20°$ (lowest plot in Fig. 3). However, we find that for elements based on those of 5025 P-L the variation in i is by no means pronounced, the amplitude being only about 7° (lower plot in Fig. 8; we have *not* plotted at the right the TC values of i, since we have shown above that secular perturbations can explain the spread). The fact that the 5025 P-L bundle remains at low inclinations will lead to close planetary encounters (which occur with a frequency that varies as $\sim 1/\sin i$) being expected rather more often than for particles in the Encke bundle. In addition, we note that the members of the 5025 P-L bundle have perihelia at ~ 0.6 au, just inside the orbit of Venus at ~ 0.7 au, so that frequent near-tangential (and hence low-speed) encounters with that planet might be anticipated, and these are effective in altering the orbits. This contrasts with the Encke bundle which comprises deep crossers of Venus, so that their encounters with the Earth and Venus are not so effective in bringing about orbital changes. It might be of interest to investigate at some stage the effect of encounters with Mercury on Encke-like orbits.

In Figs 9 and 10 we show the orbital evolution of the 18 particles based upon the orbit of (6063) Jason (the 'Jason bundle'). The results are broadly similar to those obtained for the 5025 P-L bundle, although with a smaller spread being attained. This is, at least in part, due to the higher inclinations attained by the Jason bundle (lower plot in Fig. 10), reducing the frequency of close planetary encounters and hence orbit dispersal.

From the results presented in this section we find that the effects of chaotic dynamical evolution are not sufficient to explain the dispersion in orbital elements observed in the TC, if 30 kyr (or less) is the time-scale over which that dispersion has been attained. We are therefore forced to look for another dispersal mechanism if our hypothesis of a giant comet origin for the TC asteroids is to be maintained.

3 NON-GRAVITATIONAL EFFECTS

3.1 Preamble

From the numerical integration results discussed in Section 2, in which only gravitational forces were considered, it is clear that we require a dispersion in semimajor axes to be produced by some mechanism other than gravitational effects if those same effects are to be understood to be capable of then producing the dispersion of the other elements (e and hence q, and ϖ). In Section 1 we criticized the paper by Valsecchi et al. (1995) on the (sole) grounds that their description of their results purported to address a question which was not examined. We are pleased to mention here that Valsecchi et al. (1995) *did* at least discuss the problem of the alignment of the lines of apsides of the objects that we gather into the TC (Table 1). They noted that in their long-time span (~ 1 Myr; see next paragraph) integrations the 'groupings disappear very quickly', this of course having been recognized by us and earlier by Clube & Napier (1984, 1986), thus providing the initial constraint upon the age of the TC under the giant comet hypothesis: at most 30 kyr is all the time allowed for the observed dispersion in elements. Valsecchi et al. (1995) then correctly note that three possibilities seem to exist: (i) the alignment is due to chance (cf. the low probabilities given in Section 1); (ii) the alignment is due to some selection effect yet to be identified (although in later work they do appear to have found a viable discovery selection effect: Valsecchi, personal communication); or (iii) the TC really *is* due to the very recent hierarchical disintegration of a massive progenitor. The last of those three is the explanation that we favour, at this stage. Valsecchi et al. (1995) then state that (iii) would 'imply ejection speeds of the order of many km/s, which are very hard to believe'. We believe that they have misunderstood, at that juncture, the physical processes that might be involved. What is required is that a suitable spread in semimajor axes (and hence relative speeds) be attained, but it is not a requirement of the giant comet model that these be the immediate result of some catastrophic separation between macroscopic objects; the requisite relative speeds could be built up over time, the time-scale being

© Royal Astronomical Society • Provided by the NASA Astrophysics Data System

1996MNRAS.280..806S

20–30 kyr. In passing we note that one of us (Steel 1994) has suggested that the long-standing problem of the dispersion of elements within meteoroid streams might be solved in a basically similar fashion to the mechanism that we will discuss here: upon release from a parent comet, the volatile component within meteoroids will be exposed to insolation, and anisotropic jetting of the evaporating volatiles will cause the meteoroids to take a random walk away from the cometary nucleus, thus attaining speeds relative to that nucleus which are higher than those predicted by the Whipple (1950) gas outflow model, those values being inadequate to explain the observed intrastream orbital element spreads.

In passing we note that Valsecchi et al. (1995) find that different entry corridors to Encke-type orbits (in terms of a, e, i) are possible in their $\sim$1-Myr integrations. This is equivalent to $\sim$300 000 perihelion passages for 2P/Encke, whereas most evaluations of the physical lifetimes of comets suggest that $\sim$1000 revolutions is the likely value (Fernández 1984; Ferrin & Gil 1988; Kresák & Kresáková 1990; Kresák 1990, 1991; Rickman et al. 1991). Since 2P/Encke has such a small orbit, and small perihelion distance, one might expect it to have, if anything, a physical lifetime shorter than the norm for other comets. Consequently, there is a problem in applying the dynamical findings of Valsecchi et al. (1995) to the case of 2P/Encke, unless one invokes a very long period of quiescence to that comet, perhaps caused by crustal choking of volatile loss. The non-observation of 2P/Encke before 1786 is indicative of such dormancy occurring (see below).

A way around this problem would be to suggest that the TC alignment has an origin which could be described as a hybrid of possibilities (i) and (ii) described by Valsecchi et al. (1995): the asteroid alignment is due to selection effects of some form (the asteroids being inert bodies perturbed from the main belt over $\sim$1 Myr), and the alignment of 2P/Encke (and the meteoroid stream derived from it) with the 'TC asteroids' is purely a coincidence. Although we do not favour that explanation, we point it out here as another possibility that is worthy of closer examination.

3.2 The observed non-gravitational perturbations of 2P/Encke

As might be expected from the number of returns in which they have been observed, 1P/Halley and 2P/Encke have the best-studied non-gravitational perturbations to their orbits, with the sense of the perturbations being such that at present the orbital period of 1P/Halley is increasing, whilst that of 2P/Encke is decreasing (e.g. Sitarski 1990). In this subsection it is not our intention to discuss non-gravitational effects in detail, but rather we will restrict ourselves to the pertinent facts in view of our aim, namely to explain the orbital dispersion of the TC asteroids. A recent review of cometary non-gravitational forces is that by Yeomans (1994).

The perturbations of 2P/Encke's orbit by non-gravitational forces, and how these have altered with time, have been intensively studied (e.g. Marsden & Sekanina 1974; Sekanina 1986, 1988a,b, 1990, 1993; Sitarski 1987, 1988, 1990; Festou, Rickman & Kamél 1990). For present purposes we draw attention to Sitarski's modelling of the time-variation of the rate of change of the semimajor axis ($\dot{a}$) as an asymmetric sinusoid, with a polynomial fit to the observed orbit alterations. By assuming that his five-parameter solution would hold for some centuries prior to the comet's discovery in 1786, Sitarski (1988) integrated the orbit of 2P/Encke back to 1201, and his results (if valid) may allow earlier observations of this comet to be identified: the non-observation of 2P/Encke prior to 1786 remains a mystery (Whipple & Hamid 1972; Hasegawa 1979; Sekanina 1991). Marsden & Sekanina (1974) had earlier tried to integrate the comet back to 1570, with allowance for non-gravitational effects.

A quite simple approach is taken here. For 2P/Encke there has been a monotonic decrease in a over the past $\sim$170 yr, although the rate of change has altered. We will adopt that period as a measure of the step frequency for a random walk. Actually, Sitarski's backwards extrapolation (Sitarski 1988, fig. 2) could be interpreted as justification for choosing a shorter length of time, but we will stick with 170 yr. The next thing required for the random walk calculation is the step length, which we derive from the average value of $\dot{a}$, this being $\sim 6 \times 10^{-8}$ au d^{-1} (Sitarski 1988, 1990). In 170 yr this produces a change in a of $\sim$0.0037 au, which is the step length (l). The number of steps in 30 kyr is $N = 30\,000/170$, so that the expected deviation from the origin in this assumed random walk is $N^{1/2}l = \Delta a \simeq 0.05$ au here. This is the amount that we might expect 2P/Encke to have deviated from its initial semimajor axis over 30 kyr under the action of non-gravitational forces, based upon the assumption that a random walk approach (both accelerations and decelerations occurring over a long time-base of several 10^4 yr) is appropriate. An alternative plotting of the rate of change of the semimajor axis of 2P/Encke (Sekanina 1990, fig. 16) provides support for the idea of a form of random walk process, with the trend altering as some vents open whilst others close, but with a smaller step length and higher frequency; the existence of observed discontinuous orbital anomalies for many short-period comets (Sekanina 1993) also argues in favour of this idea. Alternatively, one could assume that the semimajor axis continues to shrink at the same average rate over this long period under the action of a maintained non-gravitational deceleration – such a situation has been suggested by several authors in the past (see, e.g., Sekanina 1972; Wetherill 1991) to explain how 2P/Encke reached a sufficiently small aphelion distance so as to become decoupled from Jupiter, Sekanina (1972) suggesting that 20 kyr ago the comet was much larger and had $Q \simeq 5.2$ au, compared to the present $Q \simeq 4.1$ au – and under that circumstance one finds that $\Delta a \simeq -0.6$ au is achieved in 30 kyr. Our bottom line, then, is that over the past $\sim$30 kyr we might expect non-gravitational forces to have changed the semimajor axis of 2P/Encke by an amount between 0.05 and 0.6 au, a reasonable estimate being a few times 0.1 au. Note that this is greater than the amount of dispersion in a produced by gravitational effects (Section 2) in the Encke bundle, and about the same as the similarly derived dispersions for the 5025 P-L and Jason bundles.

It should be noted that the absence of observations of 2P/Encke (at least, none have yet been identified) in the two millennia prior to its discovery in 1786 argues against the non-gravitational forces continuing to act systematically throughout this 30-kyr period. On the other hand, the

© Royal Astronomical Society • Provided by the NASA Astrophysics Data System

1996MNRAS.280..806S

evidence from the meteor showers associated with this comet supports the occurrence of strong cometary activity over the past 20–30 kyr (Babadzhanov et al. 1990; Steel et al. 1991), and hence significant non-gravitational forces; Sekanina (1972) ended his paper by noting that 'The Taurids are perhaps the product of the comet's early violent evolution in the innermost part of the solar system'. We tend to agree, believing that the TC asteroids also resulted from that violent episode.

How does the situation for 2P/Encke reflect upon the other TC objects? Various estimates have been made of the fraction of this comet's surface which is currently losing volatile materials, the rest being mantled with dust/heavy organics. Some estimates have been extremely low (e.g. Ferrin & Gil 1988), whilst most others have suggested that perhaps 5–10 per cent of the surface is currently active (Rickman 1987, 1991). This small percentage, compared to what might be expected for a recently split comet with an interior freshly exposed to insolation, might be interpreted as implying that the Δa of a few times 0.1 au estimated above is a minimal value. If that were the case, then some objects would have been lost from the TC, assuming that they all started off with elements a, e similar to those currently occupied. This is discussed further in Section 3.4 below.

3.3 General discussion of application to the Taurid Complex asteroids

Smaller comets having the same fractional active surface area as larger comets will suffer larger non-gravitational accelerations; thus the size of 2P/Encke is pertinent. In Table 1 we listed representative diameters based on an assumed albedo $p=0.08$ for the NEAs, but for cometary nuclei the determination of a size is more problematical. A variety of techniques have been applied to 2P/Encke, including inference from the non-gravitational force (A'Hearn & Schleicher 1988; diameter $\sim$3 km derived), radar backscatter (Kamoun et al. 1982; diameter 1–8 km), dust production (Campins 1988; diameter $\sim$5 km), and optical observations near aphelion (Luu & Jewitt 1990; diameter 4.4–9.8 km for $p=0.10$–0.02). A diameter of $\sim$5 km is therefore indicated if one chooses $p=0.08$, in line with the assumption made in deriving the asteroid sizes in Table 1, and this value is not in sharp disagreement with any of the other cited evaluations of the size of the nucleus of 2P/Encke. If one now scans the TC asteroid sizes in Table 1, we find that only three of them are larger than $\sim$5 km in diameter, so that if these NEAs were behaving as active comets in the past, then we would expect larger values of Δa to result from the non-gravitational forces for most of them, assuming that their densities are similar. It therefore seems entirely feasible that non-gravitational forces could be responsible for the spread of semimajor axes between 1.8 and 2.6 au in the macroscopic TC objects. Since the non-gravitational forces are expected to have been especially substantial in the early history of the complex – larger accelerations occurring when the supposed cometary material was freshly exposed to the sunlight – it seems clear that the initial dispersal produced in this way will in any case have been amplified by the gravitational scattering through to the present era, and so the observed TC element spread shown in Figs 7 and 8 (or Figs 9 and 10) may be accommodated in this giant comet disintegration model, but not in an asteroid break-up model in which non-gravitational forces do not come into play.

This discussion has been limited to generalities based upon the dispersion to be expected in a due to non-gravitational forces, and the assertion that the dispersion in e and ϖ will follow. To show that this is indeed the case, in the next section we present the results of numerical integrations in which the influence of plausible non-gravitational forces has been accommodated.

3.4 Integrations including non-gravitational forces

In this section we present the results of some numerical integrations in which we have included modelling of plausible non-gravitational forces acting upon the test particles. Before discussing that model, we explain our choice of test particle.

Referring back to the integrations based on 2P/Encke presented in Figs 5 and 6, we note that the final eccentricities achieved are grouped around $e=0.85$, as is to be expected (given 2P/Encke's observed eccentricity). This is towards the upper limit of the values of e for the TC objects in Table 1. Similarly, the final perihelion distances achieved are in the range $0.24<q<0.40$ au, which is at the lower end of the TC values of q. Test particle orbits based directly on that of 2P/Encke might not, therefore, be the best choice for our integrations including non-gravitational forces: there is no reason to favour 2P/Encke, apart from its cometary activity observed in the current epoch (which may be merely related to its current small perihelion distance), and such high-e, low-q orbits might be preferentially lost from the complex if substantial non-gravitational forces are applied. This latter point is of interest in itself, especially from a perspective of the need for an explanation of 2P/Encke's subJovian orbit – along with all other subJovian comets, and comet-derived asteroids – and we will discuss this in a future paper.

We next turn to Figs 7 and 8, pertaining to the integrations of orbits based upon that of 5025 P-L. Although, as discussed earlier, there are some outliers, most of the 18 test particles integrated end up with values of e near 0.7, and q near 0.65 au. These are close to the central values for the TC objects, so that test particle orbits based upon 5025 P-L might be acceptable. However, examination of Figs 9 and 10 shows that the results for orbits based on (6063) Jason from those purely gravitational integrations result in final values of $e\approx0.76$ and $q\approx0.50$ au which are at least as close to the TC central values, but with a lesser spread. The larger spread in the final orbital elements produced by the 5025 P-L bundle was discussed earlier. Since in this section we are interested in discovering how large the spread produced by non-gravitational forces might be, we choose as the basis for our test-particle orbits that of (6063) Jason; that asteroid is also closer to the central value of ϖ of the TC objects than is 5025 P-L, and it has a lower value of D.

We now turn to the non-gravitational force model. As in Section 2.2, we used as an initial orbit that for (6063) Jason derived from a purely gravitational backwards integration of

© Royal Astronomical Society • Provided by the NASA Astrophysics Data System

1996MNRAS.280..806S

its present orbit to 30 kyr ago. The 18 test particles were then distributed in 20° steps in mean anomaly, as before. In Section 3.2 we discussed a random walk model for the non-gravitational forces, and here we applied perturbations based upon the same reasoning. The 18 test particles were integrated forwards to the present as usual, except that every 170 yr the semimajor axis was suddenly changed by an amount given by

$$\Delta a = \sqrt{2} X \sin\theta, \qquad (2)$$

where θ is a random angle in the range 0°–360°, and X is the modulus of the change in a. In the integrations we used two values for that modulus: $X = 0.0037$ au (based upon the currently observed non-gravitational force discussed in Section 3.2, and here referred to as being the *small* non-gravitational force), and $X = 0.0137$ au (i.e., 0.01 au or about four times bigger, and here referred to as being the *large* non-gravitational force).

The results of these integrations for the small non-gravitational force model are shown in Figs 11 and 12, which should be compared with Figs 9 and 10. The dispersions produced in all elements are rather larger than in the purely gravitational integrations, as is to be expected, but are only about 50 per cent of the spreads required in a, e and q in order to fit the observed TC object values.

Applying instead the large non-gravitational force ($X = 0.0137$ au), we obtain the results shown in Figs 13 and 14. Now that the spread in a obtained does indeed cover the full range required by the selected TC objects, the spread in e and q is about 80 per cent of that required [which we do not view as a problem, given the influence of contingency in the integrations and the fact that if we had used another base for the test orbits than (6063) Jason then quite different specific results would have been obtained], whilst the spread in ϖ is more than adequate to cover our selected TC objects. In fact, two of the test particles obtain $\varpi > 220°$ by the end of the integrations, meaning that it is feasible that the Hephaistos group (Table 1) does indeed have a common origin with the TC objects.

One criticism of the above integrations that might be made is that it has been assumed that, although the non-gravitational force is applied as an impulse once every 170 yr, nevertheless it is not to be expected that such forces would have acted throughout the 30 kyr of the integrations, else all the TC objects would be expected to appear cometary in nature now: only 2P/Encke has been identified as showing cometary activity, and that only over the past two centuries. On the other hand, an inspection of Fig. 13 shows that about 50 per cent of the dispersion in each of the elements is attained within ~10 kyr of the start of the integrations, even with a non-gravitational force applied which is quite modest in magnitude compared to the sorts of forces that might be expected for a large comet disintegrating so as to expose fragments containing rich complements of volatile material. It is not possible for us to know with certainty the precise steps through which the currently observed population of objects listed in Table 1 came about, but the simple modelling presented here supports the contention that the Taurid and Hephaistos groups are derived from just two, and possibly only one, massive cometary progenitor.

3.5 A note pertaining to the origin of subJovian orbits

One particle in Fig. 14 is clearly evolving quite differently from the others, at least from about 10 kyr ago. In Fig. 13 that particle leaves the plot for a (obtains $a > 2.6$ au) in about the year -6500, at which time the plots show that its eccentricity is reducing, and its perihelion distance is increasing. We have mentioned above that in another paper we will be examining the implications of such integrations for an understanding of the source of 2P/Encke and objects in similar orbits: this particle is one of those to be discussed there, since we find that it enters a typical Jupiter-family orbit, with aphelion $Q > 5$ au. A reversal of the arrow of time indicates that an *arrival* through such an orbit is also possible.

4 CONCLUSIONS

We have examined how particles in orbits similar to various Taurid Complex objects would have their orbital elements dispersed over 30 kyr under the action of purely gravitational effects (secular perturbations, and chaotic scattering caused by close approaches to the terrestrial planets). The results of those investigations showed that, although for some start orbits the derived scatter was appreciable, in general it is not possible to explain the spread of the TC asteroid orbits in this way alone. We therefore discussed a simple model for non-gravitational effects, based upon the observed non-gravitational perturbations of the orbit of 2P/Encke, and found that over 30 kyr this would produce a dispersion of a few times 0.1 au in the semimajor axes of the Taurid objects. If the TC is indeed the debris produced by the disintegration of a giant comet 20–30 kyr ago, then the non-gravitational perturbations would be anticipated to have been more severe soon after the fragmentation events, when volatiles would have been freshly exposed to the Sun. Numerical integrations incorporating plausible non-gravitational forces result in spreads in the orbital elements a, e and q which are similar to those of the selected TC objects, whilst the spread in ϖ is not only large enough to encompass those objects, but is also adequate to cover the Hephaistos group of objects, indicating that these might share a common origin with the former. These non-gravitational forces also provide an explanation for how 2P/Encke, and other comet-derived objects, attained a subJovian orbit. We therefore find supporting evidence for the hypothesis that the Taurid and Hephaistos groupings were produced in the hierarchical disintegration of a giant comet trapped in a subJovian orbit.

ACKNOWLEDGMENTS

We thank B. G. Marsden for helpful advice on non-gravitational forces, J. Jones for comments on the original manuscript, and S. V. M. Clube and W. M. Napier for discussions over the years. This work was supported by the Australian Research Council and the Department of Education, Employment and Training.

REFERENCES

A'Hearn M. F., Schleicher D. G., 1988, ApJ, 331, L47
Asher D. J., Bailey M. E., Hahn G., Steel D. I., 1994a, MNRAS,

© Royal Astronomical Society • Provided by the NASA Astrophysics Data System

1996MNRAS.280..806S

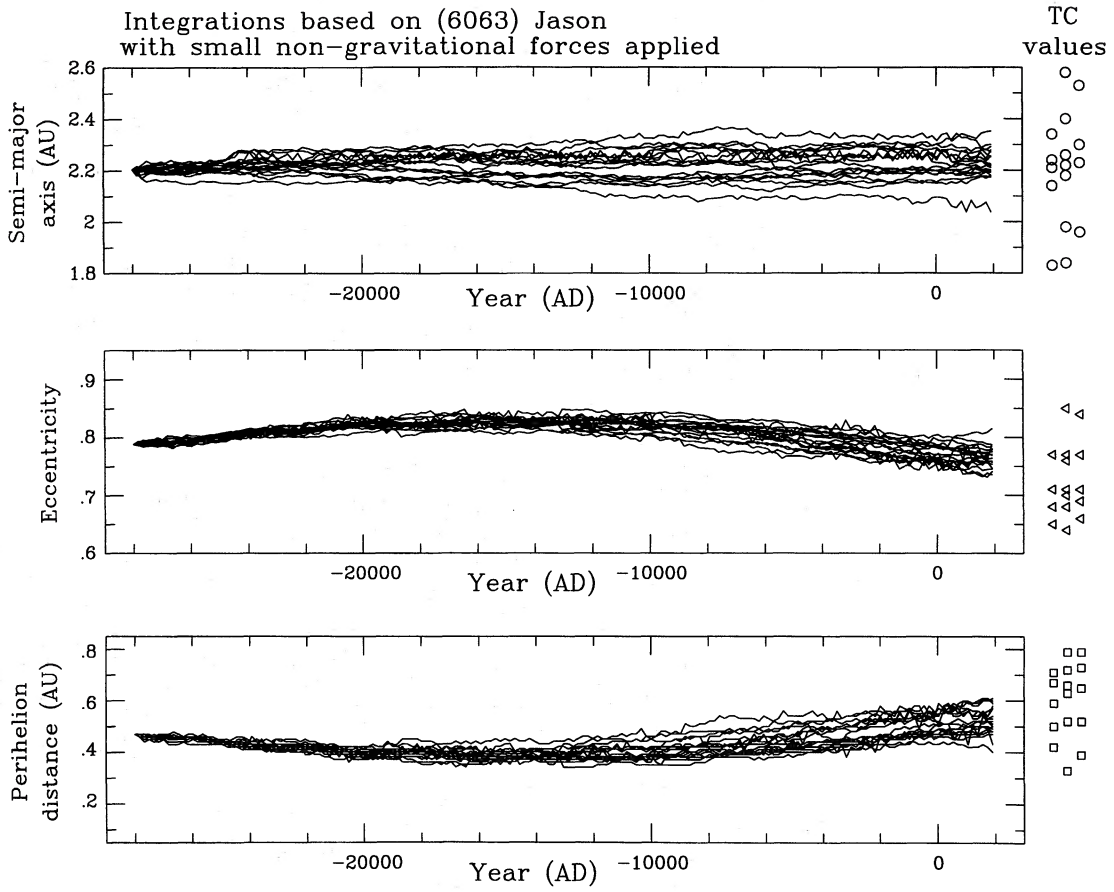

Figure 11. As Fig. 9, except for the 18 particles in the (6063) Jason bundle, now with small non-gravitational forces applied, modelled upon the non-gravitational forces of 2P/Encke observed in the present epoch. A random change in semimajor axis $\Delta a = \sqrt{2X}\sin\theta$ is applied every 170 yr, θ being a random angle in the range 0°–360° and $X = 0.0037$ au.

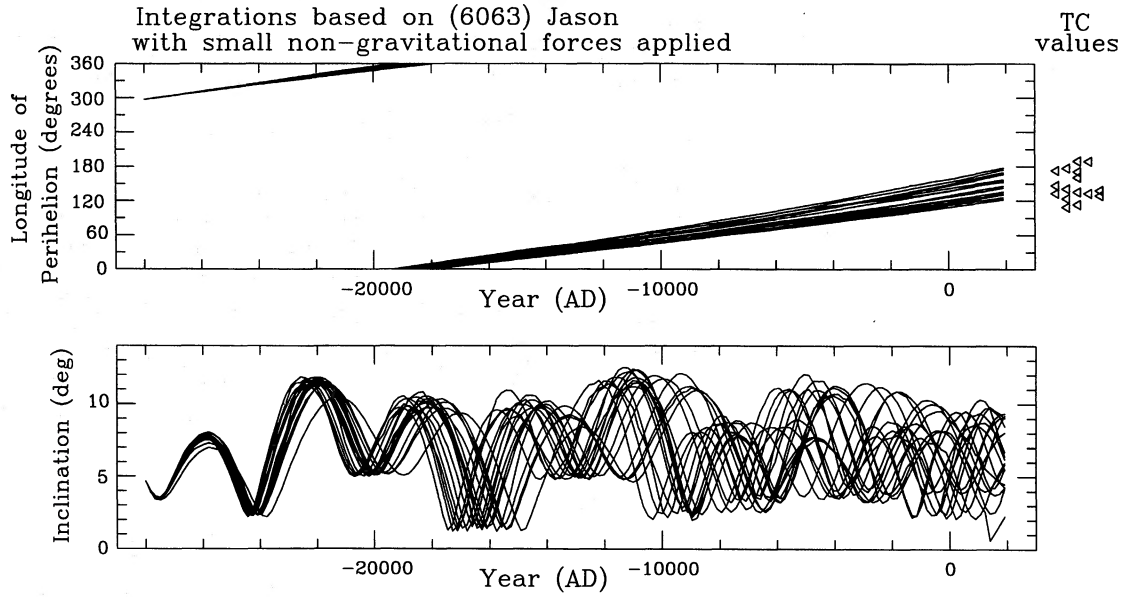

Figure 12. As Fig. 10, except for the 18 test-particle integrations shown in Fig. 11, which make use of a random walk model for the non-gravitational forces.

© Royal Astronomical Society • Provided by the NASA Astrophysics Data System

1996MNRAS.280..806S

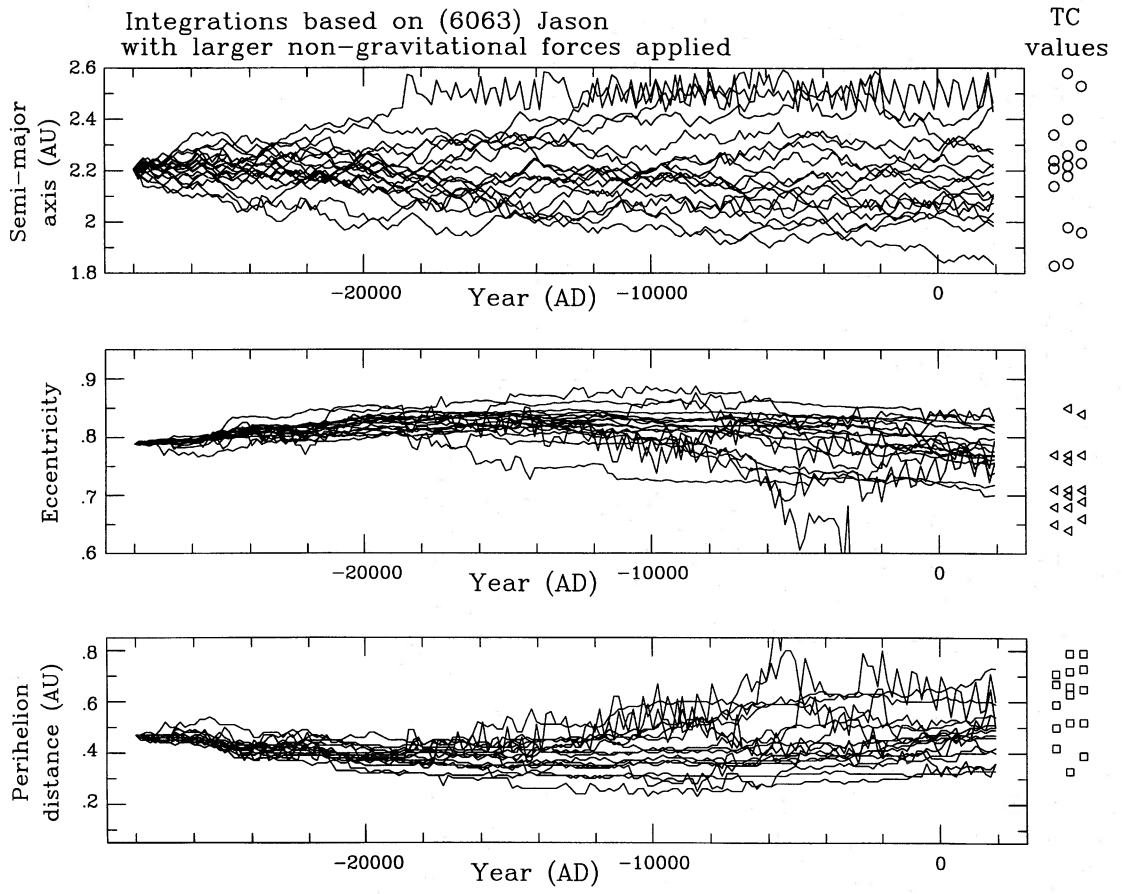

Figure 13. As Fig. 11, except with larger non-gravitational forces applied, the step length in the random walk model being $X = 0.0137$ au.

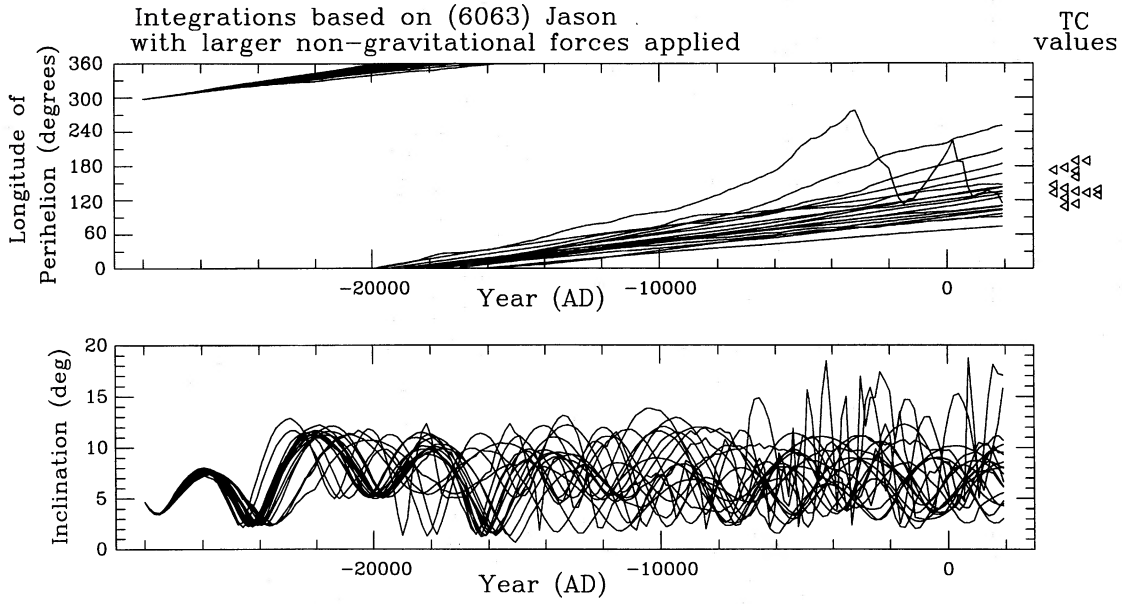

Figure 14. As Fig. 12, except for the 18 test-particle integrations shown in Fig. 13, which use larger non-gravitational forces than those in Figs 11 and 12.

© Royal Astronomical Society • Provided by the NASA Astrophysics Data System

1996MNRAS.280..806S

267, 26
Asher D. J., Clube S. V. M., 1993, QJRAS, 34, 481
Asher D. J., Steel D. I., 1993, MNRAS, 263, 179
Asher D. J., Clube S. V. M., Steel D. I., 1993a, MNRAS, 264, 93
Asher D. J., Clube S. V. M., Steel D. I., 1993b, in Štohl J., Williams I. P., eds, Meteoroids and their Parent Bodies. Slovak Acad. Sci., Bratislava, p. 93
Asher D. J., Clube S. V. M., Napier W. M., Steel D. I., 1994b, Vistas Astron., 38, 1
Babadzhanov P. B., Obrubov Yu. V., 1992, Celest. Mech. Dyn. Astron., 54, 111
Babadzhanov P. B., Obrubov Yu. V., Makhmudov N., 1990, Solar System Res., 24, 12
Brouwer D., 1947, AJ, 52, 190
Brouwer D., van Woerkom A. J. J., 1950, Astron. Papers Amer. Ephemeris, 13, 81
Campins H., 1988, Icarus, 73, 508
Clube S. V. M., 1987, Phil. Trans. R. Soc. Lond., A323, 421
Clube S. V. M., Napier W. M., 1984, MNRAS, 211, 953
Clube S. V. M., Napier W. M., 1986, in Smoluchowski R., Bahcall J. N., Matthews M. S., eds, The Galaxy and the Solar System. Univ. Arizona Press, Tucson, p. 260
Farinella P., Froeschlé Ch., Froeschlé Cl., Gonczi R., Hahn G., Morbidelli A., Valsecchi G. B., 1994, Nat, 371, 314
Fernández J. A., 1984, A&A, 135, 129
Ferrin I., Gil C., 1988, A&A, 194, 288
Festou M., Rickman H., Kamél L., 1990, Nat, 345, 235
Hahn G., Bailey M. E., 1990, Nat, 348, 132
Hasegawa I., 1979, PASJ, 31, 257
Jones J., 1986, MNRAS, 221, 257
Kamoun P. G., Campbell D. B., Ostro S. J., Pettengill G. H., Shapiro I., 1982, Sci, 216, 293
Klačka J., 1995, A&A, 295, 420
Kozai Y., 1962, AJ, 67, 591
Kresák L., 1980, in Halliday I., McIntosh B. A., eds, Proc. IAU Symp. 90, Solid Particles in the Solar System. Reidel, Dordrecht, p. 211
Kresák L., 1990, in Mason J. W., ed., Comet Halley Investigations, Results, Interpretations, Vol. 2, Dust, Nucleus, Evolution. Ellis Horwood, Hemel Hempstead, p. 259
Kresák L., 1991, in Newburn R. L., Neugebauer M., Rahe J., eds, Proc. IAU Colloq. 116, Comets in the Post-Halley Era. Kluwer, Dordrecht, p. 607
Kresák L., Kresáková M., 1987, in Rolfe E. J., Battrick B., eds, Symp. on the Diversity and Similarity of Comets, ESA SP-278, Paris, p. 739
Kresák L., Kresáková M., 1990, Icarus, 86, 82
Levison H. F., Duncan M. J., 1994, Icarus, 108, 18
Luu J., Jewitt D., 1990, Icarus, 86, 69
Marsden B. G., Sekanina Z., 1974, AJ, 79, 413
Marsden B. G., Williams G. V., 1995, Catalogue of Cometary Orbits, 10th edition. Minor Planet Center, Cambridge, MA
Michel P., Froeschlé Ch., Farinella P., 1996, Earth, Moon, Planets, 72, 151
Milani A., Carpino M., Hahn G., Nobili A. M., 1989, Icarus, 78, 212
Nakano S., 1994, Minor Planet Circ. 23483
Napier W. M., 1993, in Štohl J., Williams I. P., eds, Meteoroids and their Parent Bodies, Slovak Acad. Sci., Bratislava, p. 123
Quinn T. R., Tremaine S., Duncan M., 1991, AJ, 101, 2287
Rabinowitz D. L., 1993, ApJ, 407, 412
Rickman H., 1987, in Ceplecha Z., Pecina P., eds, Interplanetary Matter. Czechoslovak Acad. Sci., Prague, p. 37
Rickman H., 1991, Adv. Space Res., 11(6), 7
Rickman H., Froeschlé C., Kamél L., Festou M. C., 1991, AJ, 102, 1446
Rowe B. H., 1993, Sky Telesc., 85, 83
Sekanina Z., 1972, in Chebotarev G. A., Kazimirchak-Polanskaya E. I., Marsden B. G., eds, Proc. IAU Symp. 45, The Motion, Evolution of Orbits, and Origin of Comets. Reidel, Dordrecht, p. 301
Sekanina Z., 1986, AJ, 91, 422
Sekanina Z., 1988a, AJ, 95, 911
Sekanina Z., 1988b, AJ, 96, 1455
Sekanina Z., 1990, AJ, 100, 1293
Sekanina Z., 1991, J. R. Astron. Soc. Can., 85, 324
Sekanina Z., 1993, AJ, 105, 702 (erratum in AJ, 106, 401)
Sitarski G., 1987, Acta Astron., 37, 99
Sitarski G., 1988, Acta Astron., 38, 269
Sitarski G., 1990, in Mason J. W., ed., Comet Halley Investigations, Results, Interpretations, Vol. 2, Dust, Nucleus, Evolution. Ellis Horwood, Hemel Hempstead, p. 215
Steel D. I., 1994, in Milani A., Di Martino M., Cellini A., eds, Proc. IAU Symp. 160, Asteroids, Comets, Meteors. Kluwer, Dordrecht, p. 111
Steel D. I., 1995, MNRAS, 273, 1091
Steel D. I., Asher D. J., 1994, Observatory, 114, 223
Steel D. I., Asher D. J., Clube S. V. M., 1991, MNRAS, 251, 632
Steel D. I., Asher D. J., Clube S. V. M., Napier W. M., 1996, A&A, submitted
Štohl J., 1986, in Lagerkvist C.-I., Lindblad B.-A., Lundstedt H., Rickman H., eds, Asteroids, Comets, Meteors II. Univ. Uppsala, Sweden, p. 565
Štohl J., Porubčan V., 1992, in Ferraz-Mello S., ed., Proc. IAU Symp. 152, Chaos, Resonance and Collective Dynamical Phenomena in the Solar System. Reidel, Dordrecht, p. 315
Valsecchi G. B., Morbidelli A., Gonczi R., Farinella P., Froeschlé Ch., Froeschlé Cl., 1995, Icarus, 118, 169
Wetherill G. W., 1991, in Newburn R. L., Neugebauer M., Rahe J., eds, Proc. IAU Colloq. 116, Comets in the Post-Halley Era, Kluwer, Dordrecht, p. 537
Whipple F. L., 1940, Proc. Amer. Phil. Soc., 83, 711
Whipple F. L., 1950, ApJ, 111, 375
Whipple F. L., 1967, in Weinberg J. L., ed., The Zodiacal Light and the Interplanetary Medium, NASA SP-150, NASA, Washington, DC, p. 409
Whipple F. L., Hamid S. E., 1952, Helwan Obs. Bull., 41, 1
Yeomans D. K., 1994, in Milani A., Di Martino M., Cellini A., eds, Proc. IAU Symp. 160, Asteroids, Comets, Meteors. Kluwer, Dordrecht, p. 241

© Royal Astronomical Society • Provided by the NASA Astrophysics Data System